

## Article

# A Straightforward Approach to Drawing Temperature-Dependent $I$ – $V$ Curves of Solar Cell Models

Rolf Klein

Institute of Computer Science, University of Bonn, Friedrich-Hirzebruch-Allee 8, 53115 Bonn, Germany; rolf.u.klein@uni-bonn.de or rolf.u.klein@gmail.com; Tel.: +49-(0)1743241953

**Abstract:** Equivalent circuit models of solar cells are important for understanding the behavior of photovoltaic systems under different weather conditions. They provide an equation  $F(V, I) = 0$  that expresses the correspondence between voltage  $V$  and current  $I$  a cell can deliver. The performance of a cell, and, therefore, the parameters of equation  $F$ , depend on the cell's temperature and on the incoming light's energy and angle. One would like to simulate and visualize these dependencies in real time. Given a fixed set of parameters, no elementary solution  $s(V) = I$  of Equation  $F(V, I) = 0$  is known. Hence, circuit simulation systems employ numerical methods to solve this equation and to approximate the circuit's  $I$ – $V$  curve,  $C_{IV}$ . In this note, we propose a simpler approach. Instead of expressing  $I$  as a function of  $V$ , we represent both as elementary functions  $V(u)$  and  $I(u)$  of a real parameter  $u$ . In this way, the  $I$ – $V$  curve  $C_{IV}$  is obtained as the image of the mapping  $m(u) = (V(u), I(u))$  from a  $u$ -interval to the  $VI$ -plane. Our approach offers both a precise mathematical description of  $C_{IV}$  and an easy way to draw it. This allows us to study the influence of environmental changes on  $C_{IV}$  by smooth animations, and yet with rather simple means. In this paper, we consider temperature dependence as an example; changes in irradiance or angle could be incorporated as well. Using formulae suggested in the literature that describe how the parameters in equation  $F(V, I) = 0$  depend on temperature, it takes only a few lines of code to generate an interactive worksheet that shows how  $C_{IV}$ , the location of the maximum power point MPP and the maximum power change as the circuit's temperature, is altered on a slider. Such a worksheet and its location will be presented in this paper.

**Keywords:** solar cell; equivalent circuit; single-diode model; closed-form  $I$ – $V$  curve; temperature; electrothermal modeling



**Citation:** Klein, R. A Straightforward Approach to Drawing Temperature-Dependent  $I$ – $V$  Curves of Solar Cell Models. *Solar* **2022**, *2*, 509–518. <https://doi.org/10.3390/solar2040030>

Academic Editor: Vincenzo d'Alessandro

Received: 9 October 2022

Accepted: 2 November 2022

Published: 4 November 2022

**Publisher's Note:** MDPI stays neutral with regard to jurisdictional claims in published maps and institutional affiliations.



**Copyright:** © 2022 by the author. Licensee MDPI, Basel, Switzerland. This article is an open access article distributed under the terms and conditions of the Creative Commons Attribution (CC BY) license (<https://creativecommons.org/licenses/by/4.0/>).

## 1. Introduction

Solar energy is of great importance to help us reduce, and finally eliminate, the use of fossil energy. As an increasing number of photovoltaic systems are appearing in public and in private installations, knowledge of their basic properties should be made easily accessible. On this note, we attempt to take a step in this direction. Before we get started, let us look at some background information first.

Both voltage  $V$  and current  $I$  generated by a photovoltaic cell depend on the load  $L$  it has to feed. In order to compute the maximum power  $V \cdot I$  the cell can deliver to suitable  $L$ , one needs to know the mutual dependency of  $V$  and  $I$ ; that is, the  $I$ – $V$  curve  $C_{IV}$ . To this end, different models of solar cells have been suggested.

Figure 1 shows the widely used single-diode model. Here, current  $I$  delivered to load  $L$  is given by

$$I = I_{ph} - I_D - I_{sh} \quad (1)$$

A photogenetic current  $I_{ph}$  is supposed to be provided by the solar generator. Both diode current  $I_D$  and the current  $I_{sh}$  through shunt resistor  $R_{sh}$  depend on the voltage  $V_{ph}$  at the generator, which is related to  $V$  by

$$V_{ph} = V + I \cdot R_s, \quad (2)$$

taking the voltage drop at resistor  $R_s$  into account. Using the Shockley diode equation to obtain  $I_D$ , Equation (1) implies the well-known formula

$$I = I_{ph} - I_0 \cdot \left( \exp\left(\frac{V + I \cdot R_s}{n \cdot V_T}\right) - 1 \right) - \frac{V + I \cdot R_s}{R_{sh}}. \quad (3)$$

Here,  $I_0$  denotes the reverse saturation current of the diode,  $n$  equals the diode's ideality factor, and  $V_T$  stands for the thermal voltage.

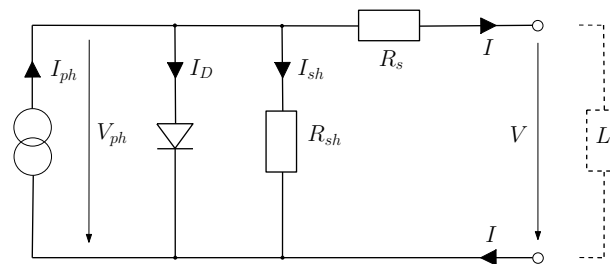


**Figure 1.** The single-diode model of a solar cell.  $I_{ph}$  denotes the photogenetic current provided by the solar generator. One part of it,  $I_D$ , passes through the diode in a forward direction. Another part,  $I_{sh}$ , runs through shunt resistor  $R_{sh}$ ; it models losses via leakage in the cell. The remaining current  $I$  passes through series resistor  $R_s$ , which represents losses caused by imperfect contacts. The values of  $I$ , voltage  $V$  and generator voltage  $V_{ph}$  depend on the load  $L$  at the cell's terminals.

Even when the values of  $V_T$ ,  $I_{ph}$ ,  $I_0$ ,  $n$ ,  $R_s$  and  $R_{sh}$  are known, the challenge is in expressing  $I$  as a function of  $V$ , or vice versa. To this end, one can rewrite (3) as equation

$$0 = F(V, I) = I_{ph} - I_0 \cdot \left( \exp\left(\frac{V + I \cdot R_s}{n \cdot V_T}\right) - 1 \right) - \frac{V + I \cdot R_s}{R_{sh}} - I. \quad (4)$$

The implicit function theorem [1] implies that there exist local solutions  $I = s(V)$  satisfying  $F(V, s(V)) = 0$  in a neighborhood of each value of  $V$ , but an explicit expression for  $s(V)$  by elementary functions (functions such as polynomials, roots, exp and ln, trigonometric functions and their inverses, and finite combinations of these are usually called elementary or of closed form) is not known. Thus, one has to resort to numerical methods.

In [2], it has been shown how to use Newton's method to approximate, for a given voltage  $V$ , the associated current  $I$ , satisfying  $F(V, I) = 0$ . The Newton method is a universal iterative algorithm for finding zeroes of smooth real-valued functions. For a sequence of  $V$ -values  $V_j$ , it can be used to approximate the associated values  $I_j$  satisfying  $F(V_j, I_j) = 0$ , with an accuracy depending on the number of iterations. Processing the values  $V_j$  one by one leads to a sequence of points  $(V_j, I_j)$  arbitrarily close to  $C_{IV}$ , but it does not provide us with a global solution  $I = s(V)$  of equation  $F(V, I) = 0$  or, vice versa, a solution  $V = r(I)$ .

Then, in [3], such a solution  $r(I)$  for  $V$  has been given in terms of the Lambert  $W$ -function,

$$W(z) \cdot \exp(W(z)) = z. \quad (5)$$

More precisely, the authors succeeded in separating the two variables  $V$  and  $I$  in (3) by providing an equation of type

$$V = r(I) = a(I, W(b(I))) \quad (6)$$

with elementary functions  $a$  and  $b$  that involve the parameters of  $F(V, I)$  but neither  $V$  nor  $I$ . Lambert function  $W$  itself is known to be *not* elementary, so that, again, it takes the Newton method or some other iterative algorithm to approximate it. However, because the  $W$  function occurs so frequently, efficient implementations of  $W(z)$  are available in advanced math systems that can be used in commercial circuit simulators. They allow  $C_{IV}$  curves to be drawn by a plot command that triggers numerous computations of  $W$  in the background.

The purpose of this paper is twofold. As a theoretical contribution, we present, in Section 3.1, an exact description of  $I$ – $V$  curves by elementary functions. Instead of writing  $I$  as a function of  $V$ , we express both as functions  $V(u)$  and  $I(u)$  of a real parameter  $u$ . In this way,  $C_{IV}$  is obtained as the image of the mapping  $m(u) = (V(u), I(u))$  from an  $u$ -interval into the  $VI$ -plane.  $V(u)$  and  $I(u)$  are directly implied by Equation (3). This approach will be described for the single-diode model; it can easily be generalized to the double-diode model and to Bishop's model [2].

Then, in Section 3.2, we derive practical benefit from our parameterization. We demonstrate that it can be used to implement, by a few lines of code, interactive tools for studying the influence of environmental parameters on  $C_{IV}$  curves. Even on a hand-held device, one can observe how a  $C_{IV}$  curve, the location of its maximum power point MPP, and the maximum power smoothly change as the circuit's temperature is altered on a slider. The influence of variable irradiance or angle could be incorporated as well.

Such tools allow research questions to be investigated using simple means. For example, there seems to be a discussion in the community as to whether the value of series resistor  $R_s$  should be modeled to grow with increasing temperature [4], or whether it could be considered constant [5]. For the parameters of a real PV module studied in [4], our simulation shows that the difference is surprisingly small. At 100 °C, power at MPP computed for increasing  $R_s$  equals 182.54 W; if  $R_s$  remains constant, peak power is larger by only 80 mW. A closer inspection of Equation (3) confirms this finding directly.

Some technical facts will be needed below. In practice, not only single cells are being considered, but also photovoltaic modules consisting of a number  $N$  of identical cells in a series circuit. Here, the single-diode model can also be applied if all cells are subjected to identical environmental parameters. In this case, thermal voltage  $V_T$  must be multiplied by  $N$  in Equation (3).

Given a real solar cell or module, one can measure its  $I$ – $V$  curve experimentally. In [6], the authors review different types of variable loads  $L$  that can be used to this end. Typically, such measurements are being taken under standard test conditions (STC), where the cell is operated at a temperature of 25° Celsius and receives an irradiance of 1000 W/m<sup>2</sup>, of light whose spectrum corresponds to an incoming angle of 48.2°. Of the parameters mentioned above, the thermal voltage is thus fixed to

$$V_T = \frac{k}{q} \cdot T = 25.7 \text{ mV}, \quad (7)$$

where  $k = 1.381 \cdot 10^{-23} \text{ J} \cdot \text{K}^{-1}$  is the Boltzmann constant,  $q = 1.602 \cdot 10^{-19} \text{ C}$  denotes the elementary charge, and  $T = 25 + 273.15$  states the absolute temperature in Kelvin.

Several methods for extracting the missing parameters  $I_{ph}$ ,  $I_0$ ,  $n$ ,  $R_s$  and  $R_{sh}$  from measurements have been reviewed in [7]. The analytic approach of [8,9] makes use of information supplied by manufacturers' data sheets, namely the values, under STC, of the open circuit voltage  $V_{oc}$ , shortcut current  $I_{sc}$ , and the maximum power point MPP. They already provide three points,  $(0, I_{sc})$ ,  $(V_m, I_m)$  and  $(V_{oc}, 0)$  on the curve  $C_{IV}$  to be constructed. Additionally, its tangent at MPP  $(V_m, I_m)$  is known to be of slope  $-I_m/V_m$ , since the derivative of  $V \cdot I$  by  $V$  must vanish at MPP. In addition, the tangent slopes of the measured curve at  $(0, I_{sc})$  and  $(V_{oc}, 0)$  can be taken. Based on these data, a satisfactory presentation of  $C_{IV}$  can be obtained [5]. In this note, we assume that the parameters at STC are given.

## 2. Electrothermal Modeling

The performance of solar cells is strongly influenced by temperature and irradiation. While irradiance measures the total radiant energy of light per unit area of a solar module, the module's performance also depends on the spectrum of the light, which is influenced by the length of the light's path through the atmosphere of Earth. The relative length of this path corresponds to the angle between this path and the line perpendicular to the Earth's surface. At  $STC$ , this angle is assumed to equal  $48.2^\circ$ .

In this paper, we focus on the influence of temperature on the power generated, assuming all other parameters are constant. To make accurate predictions, one needs to know how the parameters in (3) depend on temperature  $T$ . Then, for any given value  $T$ , curve  $C_{IV,T}$  can be computed without taking new measurements.

The behavior of the thermal voltage has already been established in (7). In [5], the authors investigate how the other five parameters of the single-diode model depend on temperature and irradiance. They are using the analytic approach and perform extensive experiments with 27 PV modules at different temperature levels. The results indicate that, for constant irradiance at  $STC$  and increasing temperature  $T$ ,

1. Diode ideality factor  $n$  can be considered constant;
2. The value of parasite resistor  $R_{sh}$  can be considered constant;
3. The value of parasite resistor  $R_s$  can be considered constant;
4. Photogenic current  $I_{ph,T}$  increases linearly with  $T$ ,

$$I_{ph,T} = I_{ph,T_{STC}} \cdot (1 + \alpha \cdot (T - T_{STC})), \quad (8)$$

proportionally to the  $\alpha$  coefficient specified in the data sheet;

5. Reverse saturation current  $I_{0,t}$  increases exponentially, as suggested in [10],

$$I_{0,T} = I_{0,T_{STC}} \cdot \left( \frac{T}{T_{STC}} \right)^3 \cdot \exp \left( \frac{1}{k} \cdot \left( \frac{E_{g,T_{STC}}}{T_{STC}} - \frac{E_{g,T}}{T} \right) \right) \quad \text{where} \quad (9)$$

$$E_{g,T} = E_{g,T_{STC}} \cdot \left( 1 - 0.0002677(T - T_{STC}) \right). \quad (10)$$

Here,  $E_g$  denotes the—also temperature dependent—energy gap; for silicon, one assumes  $E_{g,T_{STC}} = 1.12$  eV. In [5], the authors point out that there is still discussion in the literature concerning points 1., 2., and 3., while 4. and 5. seem to be accepted. In fact, in a recent paper [4] the authors assume that  $R_s$  grows linearly with temperature  $T$ ,  
3.'

$$R_{s,T} = R_{s,T_{STC}} \cdot \frac{T}{T_{STC}}. \quad (11)$$

In Section 3.2, we will discuss how the  $I$ – $V$  curve of the module studied in [4] is influenced by choosing alternative 3. or 3.'.

## 3. Results

### 3.1. Analysis

In this subsection, we develop a mathematically precise and straightforward description of  $I$ – $V$  curves that allows them to be drawn quite easily. To this end, let us start with a fixed temperature and take another look at Formula (3). The function

$$f(u) := I_{ph} - I_0 \cdot \left( \exp \left( \frac{u}{n \cdot V_T} \right) - 1 \right) - \frac{u}{R_{sh}} \quad (12)$$

is defined for every real-value  $u$ . For arguments  $u$  of special type  $u = V + I \cdot R_s$ , where  $(V, I)$  represents a point on the circuit's  $I$ - $V$  curve,  $f(u)$  becomes the right-hand side of (3), so that we obtain

$$f(u) = f(V + I \cdot R_s) = I, \quad \text{and therefore} \quad (13)$$

$$u - f(u) \cdot R_s = (V + I \cdot R_s) - I \cdot R_s = V, \quad \text{which implies} \quad (14)$$

$$(u - f(u) \cdot R_s, f(u)) = (V, I). \quad (15)$$

This means that we can obtain each point  $(V, I)$  on  $C_{IV}$  as  $(u - f(u) \cdot R_s, f(u))$  for parameter  $u = V + I \cdot R_s$  which equals  $V_{ph}$ , by (2). Hence, the appropriate range for parameter  $u$  starts with  $I_{sc}R_s$ , corresponding to point  $(0, I_{sc})$  on  $C_{IV}$ , and goes up to  $V_{oc}$  corresponding to  $(V_{oc}, 0)$ . This leads to the following result.

**Theorem 1.** *For the single-diode model of solar cells, the mapping*

$$m : [I_{sc}R_s, V_{oc}] \rightarrow \mathbf{R}^2 \quad (16)$$

$$u \mapsto (V(u), I(u)) = (u - f(u)R_s, f(u)) \quad (17)$$

*is a bijective parameterization of the  $I$ - $V$  curve  $C_{IV}$  in the first quadrant.*

The same approach works for the double-diode model [9], whose equation reads

$$I = I_{ph} - I_{0,1} \left( \exp \left( \frac{V + IR_s}{2V_T} \right) - 1 \right) - I_{0,2} \left( \exp \left( \frac{V + IR_s}{V_T} \right) - 1 \right) - \frac{V + IR_s}{R_{sh}} \quad (18)$$

and for Bishop's circuit model, which aims at modeling a cell under negative voltages by adding a second generator to the single- or double-diode model [2] (2.48). Formula (18) is then extended by another additive term

$$-b(V + IR_s) \left( 1 - \frac{V + IR_s}{V_{br}} \right)^{-a},$$

where  $b$  is a constant,  $V_{br}$  denotes the diode's breakthrough voltage, and  $a$  is called the breakthrough avalanche exponent.

Theorem 1 could be generalized to more complicated circuits, in which equation  $V$  and  $I$  are "encoded" into a single number  $g(V, I)$  more complex than  $V + IR_s$ . As long as there exist decoding functions  $f$  and  $h$  that satisfy

$$f(g(V, I)) = I \quad (19)$$

$$h(g(V, I), I) = V, \quad (20)$$

we can still obtain the following result.

**Theorem 2.** *If functions  $f, g, h$  are continuous and if  $C$  is connected, then  $g(C) = \{g(V, I); (V, I) \in C\}$  is an interval,  $C$  is a curve, and the mapping*

$$m : g(C) \rightarrow C \quad (21)$$

$$u \mapsto (h(u, f(u)), f(u)) \quad (22)$$

*is a bijective parameterization of  $C$ .*

**Proof.** The image of the connected set  $C$  under the continuous function  $g$  is again connected, hence an interval in  $\mathbf{R}$ . Mapping  $m$  is surjective because for each  $(V, I)$  in  $C$ , we know that  $g(V, I)$  lies in  $g(C)$  and that  $u = g(V, I)$  is mapped to  $(V, I)$  by  $m$ . The injectivity of  $m$  follows from the decoding property. Since  $m$  is also continuous,  $C$  must be a curve.  $\square$

In Theorem 1, the set  $C$  equals  $C_{IV}$  and  $h$  denotes the function  $h(x, y) = x - yR_s$ . We have  $g(V, I) = V + IR_s$  and  $g(C) = [I_{sc} R_s, V_{oc}]$ .

If temperature is variable, we can simply replace the constant values of  $V_T$ ,  $I_{ph}$  and  $I_0$  in the definition of  $f$  in (12) with expressions depending on  $T$  such as those discussed in Section 2 and (7), and obtain  $I$ – $V$  curves  $C_{IV,T}$ . In the same way, dependency of irradiance or angle can be incorporated. The only condition is that neither  $I$  nor  $V$  occur in these expressions other than as  $V + IR_s$ .

### 3.2. Examples

Let us start with a fixed set of parameters taken from Table 2.4 in [2],

$$I_{ph} = 1.28 \text{ A}; I_0 = 0.1659 \mu\text{A}; n = 1.375; R_s = 22 \text{ m}\Omega; R_{sh} = 20 \Omega; V_T = 25,7 \text{ mV}.$$

Even without knowing  $I_{sc}$  or  $V_{oc}$ , we can use any plotting tool to draw mapping  $m$  mentioned in Theorem 1. For a large enough range of parameter  $u$ , the output looks like the curve displayed in Figure 2. Within the first quadrant, this curve equals  $C_{IV}$ , as shown in Figure 2.5 of [2], while the rest of the curve should be ignored.

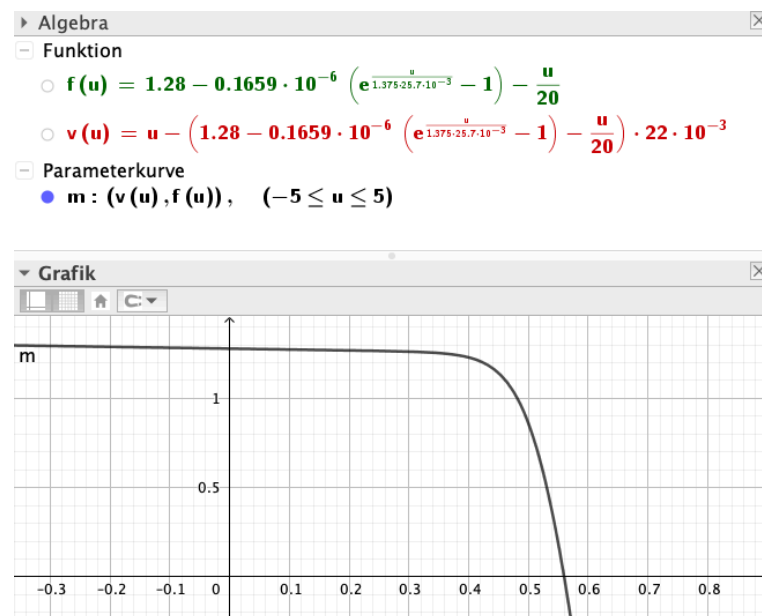


**Figure 2.** Curve  $C_{IV}$  is situated in the first quadrant.

Next, we consider the PV module studied in [4]. It consists of 60 cells, and its data sheet specifies

$$I_{ph} \approx I_{sc,T_{STC}} = 10.82 \text{ A}; \alpha = 0.04 \% / ^\circ\text{C}.$$

In their experiments, by combining numerical with analytical methods, the authors found

$$I_{0,T_{STC}} = 4.17 \cdot 10^{-8} \text{ A}; R_{s,T_{STC}} = 0.0037 \Omega; R_{sh} = 112.1 \Omega.$$

We picked the constant value  $n = 1.375$  for the diode ideality factor from a somewhat scattered cloud of measurements.

In addition to the declarations of these parameters, twelve lines of code are sufficient to generate an interactive worksheet in GeoGebra (We picked GeoGebra because it allows to manipulate dynamic geometric and algebraic objects in a very intuitive way. It is widely used in geometry research and teaching. Maple or Mathematica would be good alternatives) that draws the parameterized curve  $C_{IV,t}$  depicted in Figures 3 and 4, computes its MPP and the maximum power,  $P_t$ ; some technical details are given in the Appendix A. The dashed (blue) curve is the hyperbola  $I = h(V) = \frac{P_t}{V}$  consisting of all points  $(V, I)$  in the plane for which  $V \cdot I$  equals maximum power; it touches  $C_{IV,t}$  at MPP from the right-hand side.

In this example, it appears that the curvatures of  $C_{IV}$  and  $h$  at MPP are, up to their opposite signs, closer at high temperature than at  $STC$ . This observation raises the question of whether errors in determining the exact MPP on  $C_{IV}$  are more detrimental at lower temperature.

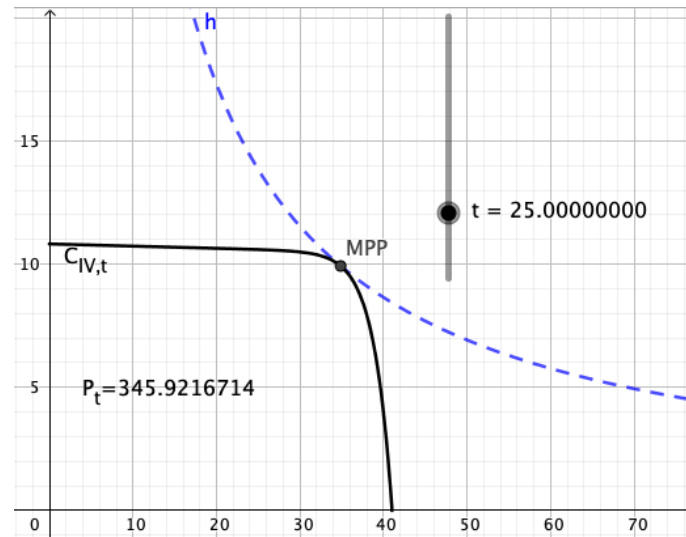


**Figure 3.** The slider allows temperature  $t$  to be changed between  $0^\circ$  and  $100^\circ\text{C}$ .

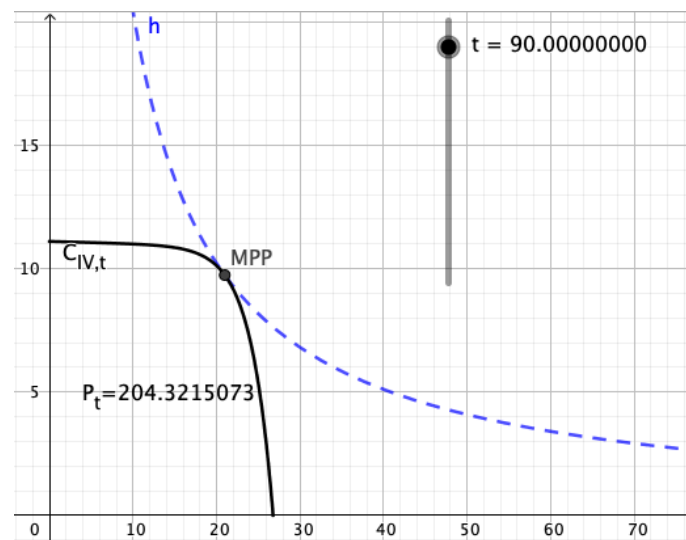


**Figure 4.** One can observe how curve  $C_{IV}$  and its MPP change; number  $P_t$  denotes the power at MPP.

Finally, we want to explore what difference it makes to have  $R_s$  linearly grow with  $T$  as opposed to fixing it at  $R_{s,T_{STC}}$ .

Figure 5 depicts the curves  $C = C_{IV,t}$  for temperature-dependent resistor  $R_s$ , and  $D = D_{IV,T_{STC}}$  for the constant value  $R_{s,T_{STC}}$ . One has to zoom in considerably to separate the two curves. Their maximum power values are quite close: 182.54 W for  $C$  and 182.62 W for  $D$ .







for the photovoltaic research community. As a side result, it could be beneficial for teaching solar systems at academic level.

**Funding:** This research received no external funding.

**Institutional Review Board Statement:** Not applicable.

**Informed Consent Statement:** Not applicable.

**Data Availability Statement:** Not applicable.

**Acknowledgments:** The author would like to thank the anonymous editor of *Solar*, the three anonymous reviewers, and Anne Brüggemann-Klein for their valuable suggestions.

**Conflicts of Interest:** The authors declare no conflict of interest.

## Appendix A

The GeoGebra software was created by Markus Hohenwarter at Linz University. It is free of charge for non-commercial use. The tool is versatile and quite powerful, and still, it is rather easy to work with. In the design of the worksheets displayed above we have made use of the following features.

First, we have specified a slider for temperature  $t$  in  $^{\circ}\text{C}$ . Its value can be used in defining algebraic objects, such as the parameterizing function  $m$ , and graphic objects such as the resulting curve; any change in  $t$  will be immediately effective in both. Clicking on the curve's points of intersection with the coordinate axes creates two new point objects,  $A$  and  $B$ . They will move along the coordinate axes as we alter the temperature. We can access their coordinates,

$$y(A) = I_{sc,t} \quad \text{and} \quad x(B) = V_{oc,t}, \quad (\text{A1})$$

and use them in defining new objects, such as the proper interval  $[I_{sc,t} R_s, V_{oc,t}]$  for parameter  $u$ , to ensure that  $C_{IV,t}$  stays in the first quadrant; see Theorem 1.

To locate MPP on  $C_{IV,t}$ , we need the maximum of the parameterized function  $P(u) = V(u) \cdot I(u)$ . GeoGebra can determine the max of functions over an interval, but not that of parameterized curves. As a workaround, we define a function  $Q(x) = V(x) \cdot I(x)$  and determine the maximum point  $m_Q$  on its graph. Then,  $y(m_Q)$  equals the maximum power and MPP has coordinates  $(V(x(m_Q)), I(x(m_Q)))$ . This can be illustrated by displaying how the hyperbola  $h(x) = y(m_Q)/x$ , the locus of all points  $(x, y)$  satisfying  $x \cdot y = y(m_Q)$ , touches  $C_{IV,t}$  at MPP. This hyperbola dynamically changes with temperature  $t$ . The worksheet can be opened and run at: (<https://www.geogebra.org/search/visualisierung%20kennlinien>, accessed on 2 November 2022) without downloading the GeoGebra system before. Individual changes to the worksheet will not overwrite the version kept on the server.

## References

1. De Oliveira, O. The implicit and inverse function theorems: Easy proofs. *Real Anal. Exch.* **2014**, *39*, 207–218. [CrossRef]
2. Quaschnig, V. *Simulation der Abschattungsverluste bei Solarelektrischen Systemen*; Verlag Dr. Köster: Berlin, Germany, 1996; pp. 28–57. Available online: <https://www.volker-quaschnig.de/downloads/abschattungsverluste.pdf> (accessed on 2 November 2022).
3. Jain, A.; Kapoor, A. Exact analytical solutions of the parameters of real solar cells using Lambert  $W$ -function. *Sol. Energy Mater. Sol. Cells* **2004**, *81*, 269–277. [CrossRef]
4. Spertino, F.; Malgaroli, G.; Amato, A.; Qureshi, M.A.E.; Ciocia, A.; Siddiqui, H. An Innovative technique for energy assessment of a highly efficient photovoltaic module. *Solar* **2022**, *2*, 321–333. [CrossRef]
5. Ruschel, S.R.; Gasparin, F.P.; Krenzinger, A. Experimental analysis of the single diode model parameters dependence on irradiance and temperature. *Sol. Energy* **2021**, *217*, 134–144. [CrossRef]
6. Durán, E.; Piliouguine, M.; Sidrach-de-Cardona, M.; Galán, J.; Andújar, J.M. Different methods to obtain the  $I$ – $V$  curve of PV modules: A review. In Proceedings of the IEEE Photovoltaic Conference, San Diego, CA, USA, 11–16 May 2008.

7. Humada, A.M.; Hojabri, M.; Mekhilef, S.; Hamada, H.M. Solar cell parameters extraction based on single and double-diode models: A review. *Renew. Sustain. Energy Rev.* **2016**, *56*, 494–509. [[CrossRef](#)]
8. Phang, J.C.H.; Chan, D.S.H.; Philips, J.R. Accurate analytical method for the extraction of solar cell parameters. *Electron. Lett.* **1984**, *20*, 406–408. [[CrossRef](#)]
9. Chan, D.S.H.; Phang, J.C.H. Analytical methods for the extraction of solar-cell single- and double-diode model parameters from  $I$ – $V$  characteristics. *IEEE Trans. Electron Devices* **1987**, *34*, 286–293. [[CrossRef](#)]
10. De Soto, W.; Klein, S.A.; Beckman, W.A. Improvement and validation of a model for photovoltaic array performance. *Sol. Energy* **2006**, *80*, 78–88. [[CrossRef](#)]